# Supporting Information

## Kranzusch et al. 10.1073/pnas.1007152107

### SI Methods

**Protein Expression and Purification.** Machupo virus cDNA (accession no. AY619642-3) was chemically synthesized (GeneArt). The *L* gene ORF was cloned with a C-terminal FLAG and 6× His tag (GGDYKDDDDKGGHHHHHH) into pFastBac Dual (Invitrogen) under the polyhedrin promoter. Mutant L SDD1328AAA was generated by QuikChange site-directed mutagenesis (Stratagene). Baculovirus was recovered by using the Bac-to-Bac system (Invitrogen), and individual plaque-purified clones were screened for optimal protein expression. *Sf*21 cells infected at an MOI of 1 were harvested 65 h post infection, and L was purified by Ni-affinity and ion exchange chromatography (GE Healthcare). Peak protein fractions were analyzed by 10% denaturing gel electrophoresis, diluted to ≈1 mg/mL and dialyzed (20 mM Tris·HCl at pH 7.0, 250 mM NaCl, 10% glycerol, and 1 mM DTT). Purified protein for structural analysis was prepared as described above except samples were diluted to ≈0.25 mg/mL, dialyzed against buffer without glycerol, stored on ice at 4 °C, and used within 24 h of infected cell harvest.

**Single-Particle Electron Microscopy Image Collection.** Images were collected on a Tecnai T12 electron microscope (FEI) equipped with an $LaB_6$ filament and operated at an acceleration voltage of 120 kV. Images were recorded on imaging plates at a magnification of 67,000× and a defocus of approximately −1.5 μm by using low-dose procedures. Imaging plates were read out with a scanner (DITABIS) by using a step size of 15 μm, a gain setting of 20,000 and a laser power setting of 30%; 2 × 2 pixels were averaged to yield a pixel size of 4.5 Å at the specimen level (1).

**RNA Probe Preparation.** A pGEM9z (Promega) transcript was generated by Sp6 (NEB) run-off transcription from SalI-linearized plasmid. RNA visualized by UV shadowing was excised from a 15% polyacrylamide-urea gel. RNA was eluted from the crushed fragment in 0.3 M NaOAc (pH 5.2) at 4 °C, extracted with phenol-chloroform, and was ethanol precipitated at −20 °C with carrier glycogen. A 7-nt 3′ RNA probe was prepared by T7 (NEB) transcription using an annealed DNA duplex (5′ TAATACGACTCACTATAG 3′ and 5′ mCmGCACAGCCCTATAGTGAGTCGTATTA 3′) with 2′-*O* methylated 5′ terminal nucleotides to promote accurate termination (2). The resulting 10-nt RNA was purified from a 20% polyacrylamide-urea gel as above. Before labeling, the 5′ triphosphate from T7 synthesized RNA probes was removed by treatment with Antarctic Phosphatase (NEB) for 30 min at 37 °C then 65 °C for 10 min.

**MACV Replicon Construction.** Plasmid pL was created by cloning L into pGEM3 (Promega). Replicon pMCm was prepared by using the backbone vector 2,0 (3). Noncoding S segment sequences were generated by overlap-extension PCR and appended to the *NP* and *eGFP* ORFs. A truncated T7 promoter with a single guanosine nucleotide flanks the 5′ end and a nonviral cytosine nucleotide followed by the HDV ribozyme sequence and T7 terminator on the 3′ end. Mutant pL and pMCm plasmids were generated by QuikChange site-directed mutagenesis (Stratagene).

**In Cell Replicon RNA Synthesis.** Confluent 6-cm dishes with $2 \times 10^6$ BSR-T7 cells were infected at an MOI of 3 with vaccinia-T7 (4). After 1 h, cells were washed and overlaid with 1.5 mL of OptiMEM including 20 μL of Lipofectamine 2000 (Invitrogen), 1 μg of pL, and 6 μg of pMCm plasmids. Cells were incubated at 37 °C for 5 h before medium was changed to DMEM supplemented with 2% FBS, 10 mM Hepes at pH 7.7, and Penicillin/Kanamycin/Streptomycin (100 units/mL; 20 μg/mL; 20 μg/mL), and cells were incubated at 34 °C for 24 h. Cells seeded on glass coverslips were washed with PBS, fixed with 10% paraformaldehyde, and mounted with AntiFade Pro (Invitrogen). Images were collected on a Zeiss Axioplan inverted fluorescent microscope.


1. Li Z, Hite RK, Cheng Y, Walz T (2010) Evaluation of imaging plates as recording medium for images of negatively stained single particles and electron diffraction patterns of two-dimensional crystals. *J Electron Microsc (Tokyo)* 59:53–63.
2. Kao C, Zheng M, Rüdisser S (1999) A simple and efficient method to reduce nontemplated nucleotide addition at the 3 terminus of RNAs transcribed by T7 RNA polymerase. *RNA* 5:1268–1272.
3. Ball LA (1992) Cellular expression of a functional nodavirus RNA replicon from vaccinia virus vectors. *J Virol* 66:2335–2345.
4. Fuerst TR, Niles EG, Studier FW, Moss B (1986) Eukaryotic transient-expression system based on recombinant vaccinia virus that synthesizes bacteriophage T7 RNA polymerase. *Proc Natl Acad Sci USA* 83:8122–8126.

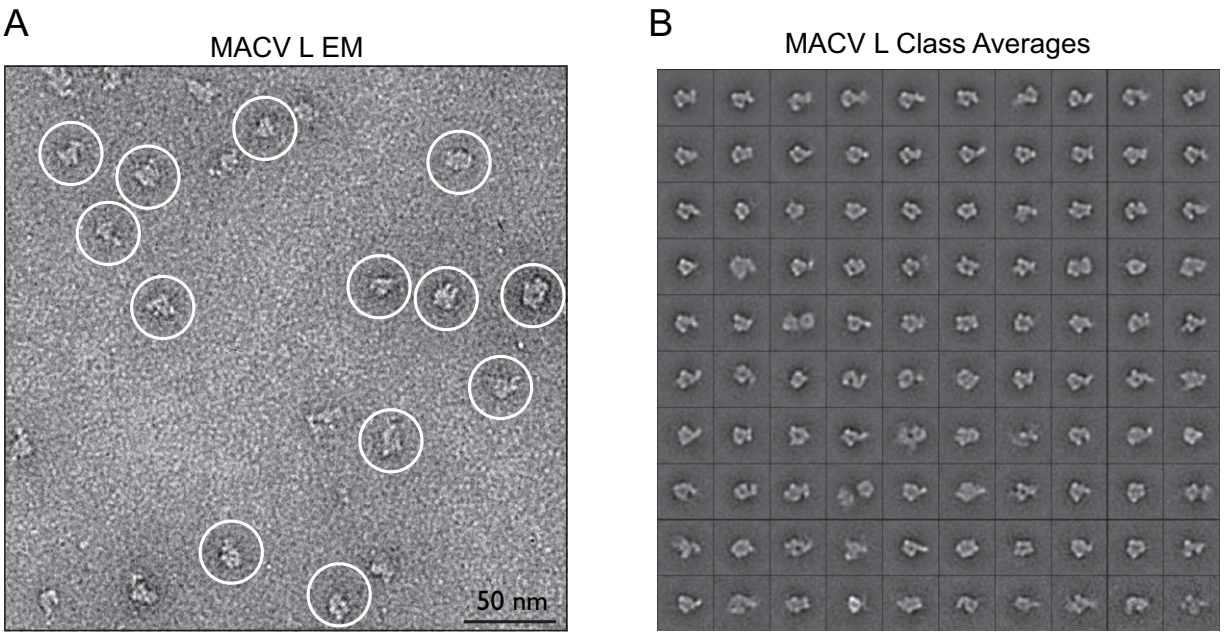


**Fig. S1.** (*A*) EM image of purified L in negative stain. (Scale bar: 50 nm.) (*B*) Class averages of negatively stained L obtained by classifying 8,871 particles into 100 classes. Class averages are arranged according to particle number such that the upper-left image represents the average with the most particles and the lower-right image contains the average with the least number of particles. Side length of the individual panels is 36 nm.

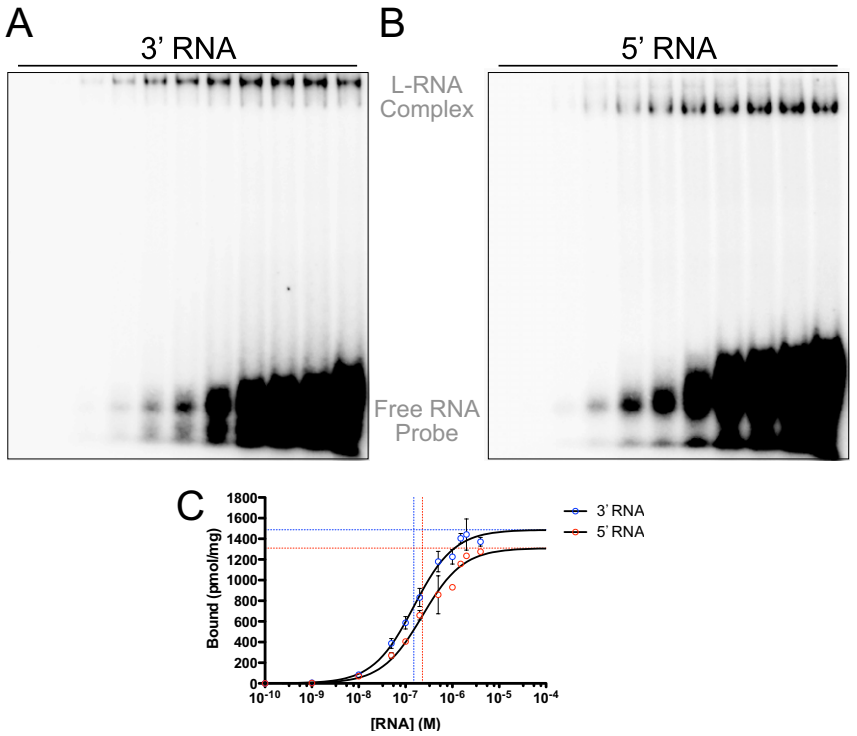


**Fig. S2.** The 3′ and 5′ RNA equilibrium saturation binding measurements. (*A* and *B*) Radiolabeled RNA ligand was titrated over a range of ≈0.01–20.0× the $K_d$ against a constant concentration of MACV L set to ensure that <10% of RNA was bound at any point to prevent ligand depletion. (*C*) Data were graphed and analyzed by one-site binding hyperbola nonlinear regression analysis. Error bars correspond to the SD from the mean of individual experiments. Vertical dashed lines correspond to the calculated $K_d$ (3′ RNA = 149.9 ± 13.12 nM and 5′ RNA = 229.1 ± 32.18 nM), and horizontal dashed lines correspond to the calculated Bmax (3′ RNA = 1,487 ± 28.19 pmol/mg and 5′ RNA = 1,309 ± 43.85 pmol/mg).

A

| RNA | Sequence | Kd Estimate |
|---|---|---|
| **3' RNA** | 1 2 3 4 5 6 7 8 9 10 11 12 13 14 15 16 17 18 19<br>3' GCGUGUCACCUAGGAUCCG 5' | **149.9 ± 13.12 nM** |
| 3' RNA 7nt | 3' GCGUGUCGGG 5' | ~200 nM |
| 3' RNA G3C | 3' GCCUGUCACCUAGGAUCCG 5' | >2 uM |
| 3' RNA Mut8-19nt | 3' GCGUGUCUGAGGCAGCUAC 5' | ~125 nM |
| **5' RNA** | 0 1 2 3 4 5 6 7 8 9 10 11 12 13 14 15 16 17 18 19<br>5' GCGCACCGGGGAUCCUAGGC 3' | **229.1 ± 32.18 nM** |
| 5' RNA Δ | 5' CGCACCGGGGAUCCUAGGC 3' | ~500 nM |
| 5' RNA 7nt | 5' GCGCACCGAAA 3' | >2 uM |
| 5' RNA 10nt | 5' GCGCACCGGGG 3' | >1 uM |
| 5' RNA 12nt | 5' GCGCACCGGGGAU 3' | >1 uM |
| 5' RNA 14nt | 5' GCGCACCGGGGAUCC 3' | >1 uM |
| 5' RNA 6-19nt | 5' AGUGGAUCCUAGGC 3' | >2 uM |
| 5' RNA Mut1-10nt | 5' GAUGCACUCAUAUCCUAGGC 3' | >1 uM |
| 5' RNA Mut8-19nt | 5' GCGCACCGAUCUGUGCGACU 3' | >1 uM |
| 5' RNA Mut11-19nt | 5' GCGCACCGGGGUGUGCGACU 3' | >1 uM |
| 5' RNA Mut13-19nt | 5' GCGCACCGGGGAUUGCGACU 3' | >1 uM |

B

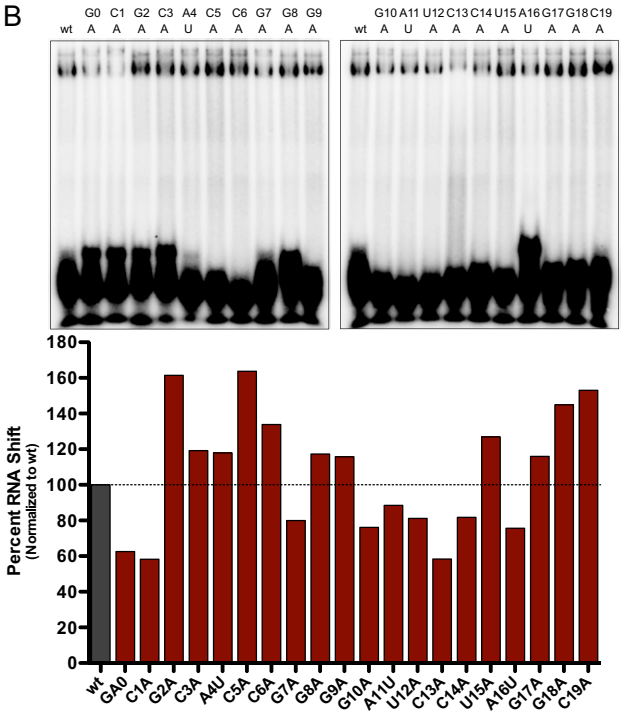


**Fig. S3.** Mutational mapping of the 3′ and 5′ RNA. (*A*) Table of tested RNA probes, sequence, and estimated affinities. $K_d$ estimates were obtained by titrating a variable range of purified L over a constant radiolabeled probe concentration of ≈$1.0 \times 10^{-10}$ M and determining the concentration of L required to shift ≈50% of input RNA. (*B*) Resulting L–RNA complexes formed with an adenosine mutagenesis panel of all 20 positions of the 20-nt 5′ RNA probe. RNA binding was quantified with a PhosphorImager and graphed as values normalized to binding of the wt 5′ RNA.

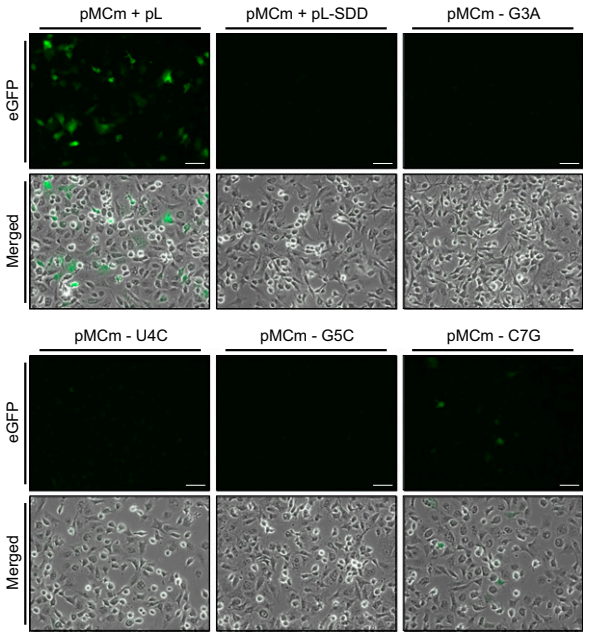


**Fig. S4.** RNA synthesis in cells correlates with L–RNA complex formation in vitro. Epifluorescence microscopy images of cells expressing the wt pMCm replicon (pMCm), replicons bearing mutations to the L 3′ RNA binding site (pMCm G3A, U4C, G5C), or a replicon with a mutation to a downstream conserved position not involved in binding (pMCm C7G). Replicons were expressed with functional MACV L (pL) or a catalytically inactivated L (pL-SDD), and eGFP-positive cells represent the cells where efficient viral RNA synthesis has occurred. (Scale bars: 50 μm.)

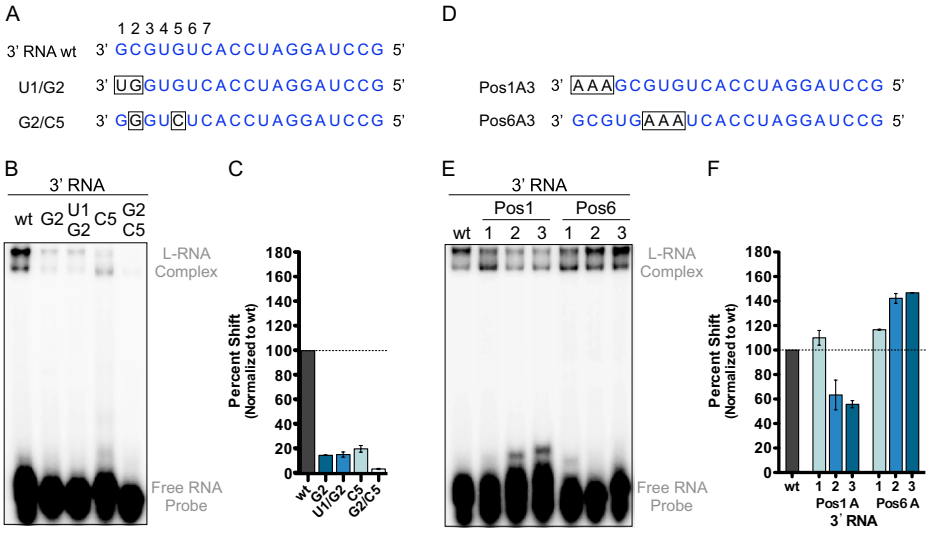


**Fig. S5.** Polymerase template recognition requires the correct positioning of the sequence element in relation to the 3′ end. (*A*) RNA probes used to analyze potential secondary structures within the 3′ termini: 19-nt RNA corresponding to the 3′ end of the S segment (3′ RNA) as well as 3′ RNA probes with paired mutations at positions 1 and 2 (3′ RNA U1/G2) or positions 2 and 5 (3′ RNA G2/C5). (*B*) The 3′ RNA probes were labeled, incubated with purified L protein, and L–RNA complexes were separated and visualized as in Fig. 3*B*. (*C*) RNA binding was quantified and graphed as in Fig. 3*C*. (*D*) RNA probes depicting 3′ RNA insertion sites used to analyze importance of binding motif proximity within the 3′ terminus: 19-nt RNA corresponding to the 3′ end of the S segment with adenosines inserted before position 1 (Pos1A1, 2, or 3) or adenosines inserted before position 6 (Pos6A1, 2, or 3). (*E*) Interaction with purified L was determined as in *B*. (*F*) Results are graphed as in *C*.

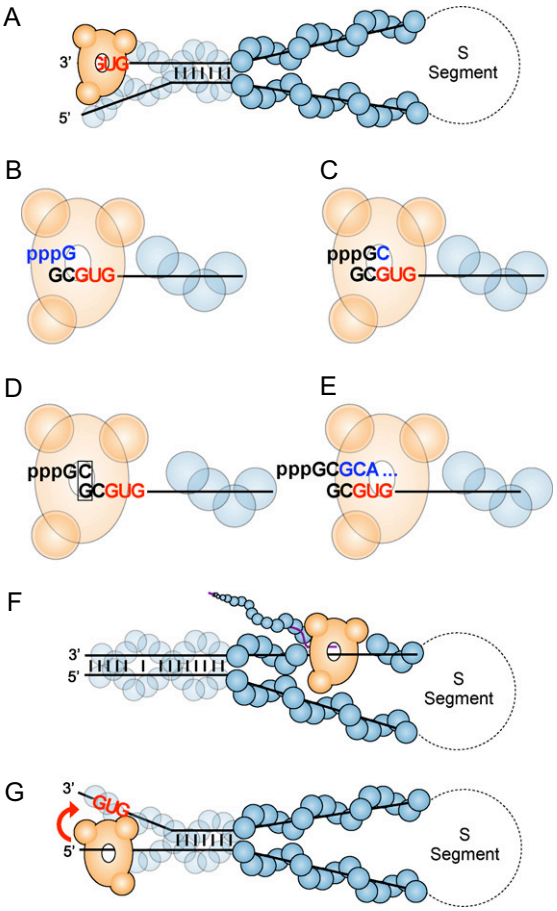


**Fig. S6.** Model of arenavirus RNA synthesis. (*A*) Cartoon diagram of the fully assembled arenavirus polymerase–template complex. (*B*) Recognition of the internal 3′ RNA binding motif facilitates accurate internal RNA synthesis initiation at position 2 of the genomic RNA. (*C* and *D*) After formation of a pppGpC primer, the polymerase template complex realigns with the extreme genomic terminus to allow faithful copying of the entire viral segment. Although the events after initiation remain unknown (*E*), once the polymerase complex moves past the promoter, inter-termini dsRNA interactions could maintain the genomic termini in close proximity (*F*), and facilitate the eventual reengagement of L with its high affinity 3′ RNA binding site and initiate a new round of RNA synthesis (*G*).